



THE UNIVERSITY *of* EDINBURGH

Edinburgh Research Explorer

Zic4-lineage cells increase their contribution to visual thalamic nuclei during murine embryogenesis if they are homozygous or heterozygous for loss of Pax6 function

Citation for published version:

Li, Z, Pratt, T & Price, D 2018, 'Zic4-lineage cells increase their contribution to visual thalamic nuclei during murine embryogenesis if they are homozygous or heterozygous for loss of Pax6 function', *eNeuro*.
<https://doi.org/10.1523/ENEURO.0367-18.2018>

Digital Object Identifier (DOI):

[10.1523/ENEURO.0367-18.2018](https://doi.org/10.1523/ENEURO.0367-18.2018)

Link:

[Link to publication record in Edinburgh Research Explorer](#)

Document Version:

Peer reviewed version

Published In:

eNeuro

General rights

Copyright for the publications made accessible via the Edinburgh Research Explorer is retained by the author(s) and / or other copyright owners and it is a condition of accessing these publications that users recognise and abide by the legal requirements associated with these rights.

Take down policy

The University of Edinburgh has made every reasonable effort to ensure that Edinburgh Research Explorer content complies with UK legislation. If you believe that the public display of this file breaches copyright please contact openaccess@ed.ac.uk providing details, and we will remove access to the work immediately and investigate your claim.



Research Article: Confirmation | Development

Zic4-lineage cells increase their contribution to visual thalamic nuclei during murine embryogenesis if they are homozygous or heterozygous for loss of Pax6 function

Ziwen Li¹, Thomas Pratt¹ and David J. Price¹

¹Simons Initiative for the Developing Brain, Biomedical Sciences, The University of Edinburgh, Hugh Robson Building, George Square, Edinburgh EH8 9XD, UK

DOI: 10.1523/ENEURO.0367-18.2018

Received: 20 September 2018

Accepted: 22 September 2018

Published: 9 October 2018

Author contributions: ZL, TP and DJP Designed Research; ZL Performed Research; ZL and DJP Wrote the paper.

Funding: <http://doi.org/10.13039/50110000265>Medical Research Council (MRC) MR/N012291/1

The authors declare no competing financial interests.

Corresponding author: David J. Price, University of Edinburgh, Hugh Robson Building, George Square, Edinburgh EH8 9XD, UK. E-mail: David.Price@ed.ac.uk

Cite as: eNeuro 2018; 10.1523/ENEURO.0367-18.2018

Alerts: Sign up at eneuro.org/alerts to receive customized email alerts when the fully formatted version of this article is published.

Accepted manuscripts are peer-reviewed but have not been through the copyediting, formatting, or proofreading process.

Copyright © 2018 Li et al.

This is an open-access article distributed under the terms of the Creative Commons Attribution 4.0 International license, which permits unrestricted use, distribution and reproduction in any medium provided that the original work is properly attributed.

1 TITLE PAGE

2
3 **Zic4-lineage cells increase their contribution to visual thalamic nuclei during murine**
4 **embryogenesis if they are homozygous or heterozygous for loss of Pax6 function**5
6 Abbreviated title: Pax6 affects *Zic4*-lineage in developing thalamus7
8 Ziwen Li, Thomas Pratt, David J.Price9 Simons Initiative for the Developing Brain, Biomedical Sciences, The University of Edinburgh, Hugh Robson
10 Building, George Square, Edinburgh EH8 9XD, UK11
12 Corresponding author:

13 David J. Price, University of Edinburgh, Hugh Robson Building, George Square, Edinburgh EH8 9XD, UK

14 David.Price@ed.ac.uk15 Author contributions: ZL, TP and DJP Designed Research; ZL Performed Research; ZL and DJP Wrote the
16 paper17
18 Number of pages: 25

19 Number of figures: 12

20 Number of tables: 0

21 Number of words for Abstract: 185

22 Number of words for Introduction: 442

23 Number of words for Discussion: 975

24
25 Conflict of Interest: The authors declare no competing financial interests.26
27 This work was supported by Medical Research Council MR/N012291/1 to DJP and an Edinburgh University
28 Global Research Scholarship and Principal's Career Development Scholarship to ZL. We thank the staff at
29 the University of Edinburgh for invaluable help with mouse maintenance; Thomas Theil and Nicoletta
30 Kessarlis for the *Zic4^{Cre}* mice; Nicoletta Kessarlis for the *Zic4* plasmids; Dr Martine Manuel for advising and
31 colony managing; Anisha Kubasik-Thayil for helping with confocal microscopy; Vivian Alison and Louis Dunn
32 for helping with histology; Mike Molinek for supervising the laboratory work.33
34 Funding: Medical Research Council MR/N012291/1 to DJP and an Edinburgh University Global Research
35 Scholarship and Principal's Career Development Scholarship to ZL.

40 ***Zic4*-lineage cells increase their contribution to visual thalamic nuclei during murine**
41 **embryogenesis if they are homozygous or heterozygous for loss of *Pax6* function**

42

43 Abbreviated title: Pax6 affects *Zic4*-lineage in developing thalamus

44

45 Ziwen Li, Thomas Pratt, David J.Price

46 Simons Initiative for the Developing Brain, Biomedical Sciences, The University of Edinburgh, Hugh Robson
47 Building, George Square, Edinburgh EH8 9XD, UK

48

49 Corresponding author:

50 David J. Price, University of Edinburgh, Hugh Robson Building, George Square, Edinburgh EH8 9XD, UK

51 David.Price@ed.ac.uk

52

53 Number of pages: 25

54 Number of figures: 12

55 Number of tables: 0

56 Number of words for Abstract: 185

57 Number of words for Introduction: 442

58 Number of words for Discussion: 975

59

60 Conflict of Interest: The authors declare no competing financial interests.

61

62 This work was supported by Medical Research Council MR/N012291/1 to DJP and an Edinburgh University
63 Global Research Scholarship and Principal's Career Development Scholarship to ZL. We thank the staff at
64 the University of Edinburgh for invaluable help with mouse maintenance; Thomas Theil and Nicoletta
65 Kessaris for the *Zic4^{Cre}* mice; Nicoletta Kessaris for the *Zic4* plasmids; Dr Martine Manuel for advising and
66 colony managing; Anisha Kubasik-Thayil for helping with confocal microscopy; Vivian Alison and Louis Dunn
67 for helping with histology; Mike Molinek for supervising the laboratory work.

68 **Abstract**

69 Our aim was to study the mechanisms that contribute to the development of discrete thalamic nuclei
70 during mouse embryogenesis (both sexes included). We characterized the expression of the transcription
71 factor coding gene *Zic4* and the distribution of cells that expressed *Zic4* in their lineage. We used genetic
72 fate mapping to show that *Zic4*-lineage cells mainly contribute to a subset of thalamic nuclei, in particular
73 the lateral geniculate nuclei, which are crucial components of the visual pathway. We observed that almost
74 all *Zic4*-lineage diencephalic progenitors express the transcription factor Pax6 at variable location-
75 dependent levels. We used conditional mutagenesis to delete either one or both copies of *Pax6* from *Zic4*-
76 lineage cells. We found that *Zic4*-lineage cells carrying either homozygous or heterozygous loss of *Pax6*
77 contributed in abnormally high numbers to one or both of the main lateral geniculate nuclei. This could not
78 be attributed to a change in cell production and was likely due to altered sorting of thalamic cells. Our
79 results indicate that positional information encoded by the levels of Pax6 in diencephalic progenitors is an
80 important determinant of the eventual locations of their daughter cells.

81

82 **Significance Statement**

83 The development of the thalamus is a process in which cells that initially appear similar give rise to distinct
84 cell groups called nuclei. How these nuclei form is poorly understood. We utilised a mouse model in which
85 cells that express the gene *Zic4* can be followed. We studied the consequences of knocking out either one
86 or both copies of the gene encoding the Pax6 transcription factor in these *Zic4*-lineage cells. We found that
87 these mutations had significant effects on the contribution of *Zic4*-lineage cells to specifically visual
88 thalamic nuclei. This was not attributable to a change in *Zic4*-lineage cell production in mutants. Rather, we
89 suggest that mutation of Pax6 affects the distribution of *Zic4*-lineage neurons to specific thalamic nuclei.

90 **Introduction**

91 The diencephalon is one of the two major components of the vertebrate forebrain. It contains several
92 structures essential for brain function, including the thalamus and prethalamus. The thalamus is an
93 important regulator of fundamental processes including sleep, alertness, consciousness and cognition, and
94 is involved in the regulation of cortico-cortical communication and the relaying of sensory information to
95 the cerebral cortex (Jones 2007; Sherman and Guillery, 2002, 2006, 2011). The thalamus is commonly
96 subdivided into more than 40 distinct nuclei, distinguished according to their function, cytoarchitecture,
97 anatomical connectivity and gene expression patterns (Jones, 2007; Martinez-Ferre and Martinez, 2012;
98 Lim and Golden, 2007). For example, the lateral geniculate nucleus (LGN) is essential for the processing of
99 visual information. The LGN is divided into two major components: the dorsal lateral geniculate nucleus
100 (dLGN) relays visual signals from the retina to the visual cortex; the ventral lateral geniculate nucleus
101 (vLGN) is involved in processing and integration, having inputs from retina, cortex and superior colliculus
102 and connections to other thalamic nuclei.

103 Thalamic nuclei develop in the mouse embryo during the final third of gestation as neurons generated from
104 progenitors lining the third ventricle migrate radially into the thalamic mantle zone (Nakagawa and
105 Shimogori, 2012). This process is likely to be regulated by the transcription factor Pax6, which is expressed
106 by most diencephalic progenitors. The relatively few exceptions are located at the zona limitans
107 intrathalamica (ZLI) between the thalamus and prethalamus (Ericson et al., 1997, Macdonald et al., 1995,
108 Robertshaw et al., 2013; Caballero et al., 2014). The expression level of Pax6 varies systematically across
109 the thalamus from high (caudally) to low (rostrally) and is high in the prethalamus. It can, therefore, confer
110 positional identity on diencephalic progenitors, which might contribute to the ability of their daughter
111 neurons to coalesce into discrete nuclei later in development.

112 *Zic4* is a zinc finger transcription factor expressed in embryonic mouse nervous system, including the
113 diencephalon, from embryonic day (E) 9.5 on (Aruga et al., 1996a,b; Gaston-Massuet et al., 2005). A
114 previous study reported that it is highly expressed in the postnatal LGN (Horng et al., 2009). We began our
115 study by testing whether cells related by the expression of *Zic4* at some time in their lineage (referred to as

116 *Zic4*-lineage cells) contribute selectively to specific thalamic nuclei. We carried out a detailed analysis of the
117 development of both *Zic4* expression and the distributions of *Zic4*-lineage cells in the embryonic
118 diencephalon and found that *Zic4*-lineage cells are distributed preferentially to a select subset of thalamic
119 nuclei, in particular the vLGN, by the time of birth. We then studied the consequences of *Zic4*^{Cre} induced
120 deletions of either one or both copies of *Pax6*.

121

122 **Materials and Methods**

123 Mice

124 All experiments were conducted in accordance with Home Office UK regulations and University of
125 Edinburgh animal welfare guidelines.

126 Conditional *Pax6* knockout mice were generated by crossing floxed *Pax6* mutant mice *Pax6*^{fl/fl} (Simpson et
127 al., 2009) with *Zic4*^{Cre} mice (Rubin et al., 2010), a kind gift from Dr Thomas Theil at Centre for Discovery
128 Brain Sciences at the University of Edinburgh. These mice were crossed with *RCE:loxP* mice (Miyoshi et al.,
129 2010) to report the Cre activity with the expression of an enhanced green fluorescent protein (EGFP,
130 subsequently referred to as GFP). The triple transgenic mice were maintained on a C57BL/6 background. To
131 obtain *Zic4*^{Cre+/-};*Pax6*^{fl/fl};*RCE*^{+/-}, *Zic4*^{Cre+/-};*Pax6*^{fl/+};*RCE*^{+/-} and *Zic4*^{Cre+/-};*Pax6*^{+/+};*RCE*^{+/-} embryos (subsequently
132 referred to as *Pax6*^{fl/fl}, *Pax6*^{fl/+} and *Pax6*^{+/+}), *Pax6*^{fl/+};*RCE*^{+/-} females were crossed with *Pax6*^{fl/+};*Zic4*^{Cre+/-} males.
133 To obtain *Zic4*^{Cre+/-};*RCE*^{+/-} embryos, *RCE*^{+/-} females were crossed with *Zic4*^{Cre+/-} males.

134 Genotyping

135 *Zic4*^{Cre+/-} mice were genotyped using primers (forward: GAGGGACTACCTCCTGTACC, reverse:
136 TGCCCAGAGTCATCCTTGGC) to the *iCre* cassette (Rubin et al., 2010), resulting in a 630 bp PCR product in
137 the mutant. *RCE*^{+/-} mice were genotyped using three primers (Rosa1: CCCAAAGTCGCTCTGAGTTGTTATC;
138 Rosa2: GAAGGAGCGGGAGAAATGGATATG and Cag3: CCAGGCGGGCCATTACCGTAAG) to the EGFP reporter
139 (Miyoshi et al., 2010), resulting in a 550 bp PCR product in the wild type and a 350 bp PCR product in the
140 mutant. Mice carrying the *Pax6*^{fl} transgene (Simpson et al., 2009) were genotyped using two primers

141 (FP6GtF: AAATGGGGTGAAGTGTGAG, FP6GtR: TGCATGTTGCCTGAAAGAAG), resulting a 156 bp PCR
142 product in the wild type and a 195 bp PCR product in the mutant.

143 All *Zic4*^{Cre+/-};*RCE*^{+/-} embryos and pups were distinguished from wild type mice based on the detection of the
144 GFP reporter using a GFP stereoscope and genotyped for the *Pax6*^{fl} transgene using the primers described
145 above.

146 Tissue preparation and histology

147 The day that the vaginal plug was found was considered as embryonic day 0.5 (E0.5). For postnatal studies,
148 the birth date was considered as postnatal day 0 (P0). Embryos were extracted from pregnant females by
149 caesarean section following an overdose of isoflurane and were harvested into ice cold phosphate buffered
150 saline (PBS). For embryos aged from E11.5 to E14.5, whole heads were removed and fixed in 4% (w/v)
151 paraformaldehyde (PFA) in PBS overnight at 4°C. For embryos aged from E15.5 to E18.5, brains were
152 dissected from skulls before proceeding to fixation. P0 pups were anaesthetised by an overdose of sodium
153 pentobarbitone and perfused with 4% PFA through the left ventricle of the heart. The brains were
154 extracted and immersed in 4% PFA for 48 hours at 4°C.

155 Fixed samples were either dehydrated in 70% EtOH and embedded in paraffin for microtome sectioning or
156 cryo-protected in 30% sucrose (w/v) in PBS, embedded in a 1:1 mixture of 30% sucrose (w/v) in PBS and
157 optimal cutting temperature (OCT) compound (Tissue-Tek, Sakura Finetek Europe, The Netherlands), and
158 frozen on dry ice for cryostat sectioning. All samples were sectioned coronally at 10 µm.

159 Fluorescent *in situ* hybridisation

160 The digoxigenin (DIG)-labelled *Zic4* antisense RNA probe was used at a concentration of 1:2000.
161 Fluorescent *in situ* hybridisations were performed according to a published protocol (Rubin et al., 2010).
162 The plasmid used to generate the *Zic4* probe was the IMAGE clone 6400880 (linearised with EcoRI and
163 transcribed with T3 RNA polymerase), a kind gift from Professor Nicoletta Kessar, Wolfson Institute for
164 Biomedical Research, University College London, UK.

165 Immunohistochemistry

166 Fluorescent immunohistochemistry was performed on paraffin embedded sections according to previously
167 published protocols (Martynoga et al., 2005). Diaminobenzidine (DAB) immunohistochemistry for Pax6 was
168 performed using the Vectastain ABC kit (Vector Laboratories, Peterborough, UK) following an incubation of
169 slides in biotinylated secondary antibodies and slides were incubated in 3% hydrogen peroxide/90%
170 methanol for 30 min to inactivate endogenous peroxidase activities during the rehydration process.

171 Primary antibodies used were as follow: mouse anti-BrdU IgG1 (1:150, BD Biosciences, RRID:AB_10015219),
172 rabbit anti-Ki67 IgG (1:500, Abcam, RRID:AB_2049848), rabbit anti-pHH3 (Ser10) (1:100, Millipore,
173 Burlington, Massachusetts, USA), mouse anti-Tuj1 IgG (1:400, Abcam, Cambridge, UK), goat anti-GFP IgG
174 (1:150, Abcam), mouse anti-COUP-TFI IgG_{2A} (1:500, R&D System, RRID:AB_1964211), mouse anti-COUP-TFII
175 IgG_{2A} (1:1000, R&D System, RRID:AB_1964214), mouse anti-LIM1/2 (1:50, Developmental Studies
176 Hybridoma Bank [DSHB], University of Iowa, USA), mouse anti-Nkx2.2 (1:200, DSHB), mouse anti-Pax6
177 (AD2.38) (a kind gift from Professor Veronica Van Heyningen at Institute of Genetics and Molecular
178 Medicine, University of Edinburgh).

179 Secondary antibodies used were donkey anti-goat Alexa Fluor 488 (1:200, Invitrogen, Carlsbad, California,
180 USA), rabbit anti-mouse biotin (1:200, Vector Laboratories, Peterborough, UK), goat anti-rabbit biotin
181 (1:200, Vector Laboratories), Streptavidin Alexa Fluor 594 (1:200, Invitrogen), donkey anti-mouse Alexa
182 Fluor 568 (1:200, Invitrogen), donkey anti-mouse Alexa Fluor 647 (1:200, Invitrogen), donkey anti-rabbit
183 Alexa Fluor 647 (1:200, Invitrogen).

184 Bromodeoxyuridine (BrdU) labelling

185 A single dose of BrdU (70 µg/g mouse weight, diluted in saline 10 µg/µl) was administrated via
186 intraperitoneal injection to pregnant dams carrying E10.5, E11.5, E12.5 and E13.5 embryos. For birthdate
187 studies, brain tissue was collected from four P0 *Zic4Cre^{+/+};RCE^{+/+};Pax6^{+/+}* pups for each injection age (E10.5 –
188 E13.5). For cell proliferation studies, four embryos were collected for brain tissue 1.5 h after injection for
189 each injection age (E11.5 – E12.5).

190 Imaging, image processing and cell counting

191 DAB images were taken with a Leica DFC480 camera connected to a Leica DMNB epifluorescence
192 microscope. Fluorescence images were taken with a Leica DM5500B automated upright microscope
193 connected to a DFC360FX camera and a Nikon A1R confocal microscope.

194 For birthdating studies, vLGN, dLGN and ventral posterior (VP) nuclei were outlined and processed in
195 CellProfiler (Lamprecht et al., 2007) using a custom pipeline. RGB images were split into three single-
196 channel grey scale images and a global thresholding was performed to reduce background noises. Cell
197 nuclei were identified using DAPI staining and a cut-off intensity value of 5 was used to distinguish nuclei
198 with positive or negative staining for both BrdU and GFP. All cell nuclei were classified and automatically
199 counted into four categories: GFP-BrdU-, GFP-BrdU+, GFP+BrdU+ and GFP+BrdU- and proportions of each
200 category were calculated and exported into spreadsheets.

201 For cell proliferation studies, a box with a fixed width was positioned and stretched to include the whole
202 diencephalic wall for three structures of interest: the prethalamus and the pTH-R and pTH-C in the
203 thalamus. Cropped images were processed in CellProfiler. Cell nuclei segmentation and fluorescence
204 intensity measurements for BrdU, pHH3, Ki67, Tuj1 and GFP were performed as described above, with the
205 same intensity cut-off applied ahead of cell counting.

206 For cell contribution studies, volumes of vLGN, dLGN and VP were estimated using the ImageJ Volumest
207 plugin (Merzin, 2008) using a series of ten coronal sections with a regular interval of 60 μm . Within each
208 section, nuclei were outlined and overlaid with a counting grid. 30% of counting tiles (30 μm x 30 μm)
209 were randomly sampled using a custom ImageJ plugin (inspired by Wayne Rasband's ImageJ plugin Grid)
210 and manually counted to calculate densities of all cells and GFP+ cells. The number of all cells in each
211 nucleus was calculated by multiplying its volume and cell density.

212 Code accessibility

213 Custom CellProfiler pipeline and ImageJ sampling tile generator plugin will be provided upon request.

214 Statistical analyses

215 Statistical analyses were conducted using the Prism 7 statistical software (Version 7.01, GraphPad Software
216 Inc.). Univariate statistics (means \pm SEM) were performed for all studied variables. One-way ANOVA was
217 performed to study the effect of genotype and two-way ANOVA was performed to examine the effects of
218 genotype and anterior-posterior position. The Tukey post hoc test was performed for all pair-wise
219 comparisons subsequent to the ANOVAs.

220

221 Results

222 *Zic4* and *Zic4^{Cre}* expression in the embryonic diencephalon

223 We began by thoroughly analysing and comparing the expression of *Zic4* transcripts and GFP reporter in the
224 *Zic4Cre^{+/+};RCE^{+/-}* diencephalon at embryonic stages from E11.5 to birth (Figs. 1-3). Whereas in situ
225 hybridizations for *Zic4* mRNA revealed the expression patterns of the gene at the time of analysis, GFP
226 revealed cells that were either expressing or at some time in their past expressed *Zic4* (*Zic4*-lineage cells).

227 In the E11.5 diencephalon (Fig. 1A-F), *Zic4* transcripts were detected at highest levels in cells of the
228 prethalamus (Fig. 1C1,D1) and the eminentia thalami (Fig. 1B1). In the prethalamus, the *Zic4* transcripts
229 were concentrated in cells on the outer, pial side of the neuroepithelium (Fig. 1E). GFP expression
230 overlapped that of *Zic4* transcripts, with GFP+ cells most frequent in the prethalamus and the eminentia
231 thalami (Fig. 1B2,C2,D2). GFP reporter activity did not correspond perfectly to the expression of *Zic4*
232 transcripts, with many *Zic4*+ cells being GFP negative (Fig. 1E,F). The most likely explanation for this was
233 that insufficient time had elapsed following the onset of *Zic4* expression for the production of detectable
234 levels of GFP. This delay would have been for the production of Cre recombinase from the *Zic4Cre*
235 transgene, the consequent activation of the reporter gene and the production of sufficient GFP.

236 At E12.5, *Zic4* transcripts were present more widely, from epithalamus through thalamus and prethalamus
237 to eminentia thalami (Fig. 1H1-J1). Expression levels were still highest in the prethalamus, as at E11.5, but
238 were also strong in the epithalamus. In the thalamus, expression levels were highest in more anterior
239 sections. GFP expression showed very similar patterns (Fig. 1H2-J2).

240 These E12.5 patterns of *Zic4* and GFP expression were largely maintained as the tissues grew in size over
241 subsequent days up to birth (Figs. 2,3). As thalamic nuclei formed during this period, *Zic4*/GFP+ cells
242 became concentrated in the vLGN, around the border between the thalamus and prethalamus, in anterior
243 thalamic regions and in the epithalamus. By birth, the densest concentration of GFP+ *Zic4*-lineage cells was
244 in vLGN and the medial habenula of the epithalamus (Fig. 3H,I). Their densities were intermediate in other
245 lateral thalamic nuclei such as the dLGN and in the zona incerta of the prethalamus. They were low in
246 midline thalamic nuclei such as nucleus reuniens and the rhomboid nucleus, and almost absent from
247 ventral posterior thalamic nuclei such as the ventral posterolateral nucleus (VPL) and ventral posteromedial
248 nucleus (VPM) (Fig. 3H,I).

249 These findings indicate that *Zic4*-lineage diencephalic progenitors contribute their daughter cells mainly to
250 the thalamic nuclei that are close to the boundary between thalamus and prethalamus, particularly to the
251 vLGN but also to others such as the dLGN.

252 **Overlap between *Zic4*-lineage and Pax6 expressing cells**

253 The normal expression pattern of Pax6 is shown at E12.5, E13.5, E14.5 and E16.5 in Figs. 4A1-F1,5A1-
254 G1,6A1-G1,7A1-F1. Pax6 is expressed at some level in almost all progenitors throughout the epithalamus,
255 thalamus, prethalamus and eminentia thalami, the exceptions being located in the ZLI, a small strip of
256 tissue between the thalamus and prethalamus (Fig. 4E1). In thalamus, it is distributed in a gradient with the
257 lowest levels close to the border with the prethalamus (Figs. 4A1-E1, 5A1-E1). Since it is not expressed by
258 postmitotic thalamic neurons, it almost completely disappears once the progenitor population is exhausted
259 by E16.5 (Fig. 7A1-F1).

260 In the prethalamus, Pax6 is strongly expressed by progenitors and is retained by many postmitotic cells as
261 they migrate radially into the diencephalic mantle zone (Figs. 4A1-E1, 5A1-E1, 6A1-G1). These cells form a
262 Pax6-positive strip running across the prethalamus. At early stages, some of them migrate as far as the
263 outer edge of the neuroepithelium to a region where the vLGN will form (Fig. 5B1-E1,G1). By E14.5, when
264 the development of discrete diencephalic nuclei is underway, most Pax6-expressing cells are located in the

265 zone incerta (ZI) of the prethalamus (Fig. 6A1-G1). At E14.5 and E16.5, we observed small numbers of Pax6-
266 expressing cells in the vicinity of the vLGN, mostly around rather than within it (Fig. 6E1-G1, 7D1-F1).

267 As expected, given that Pax6 is expressed by almost all thalamic and prethalamic progenitors, double-label
268 experiments showed that *Zic4*-lineage thalamic and prethalamic progenitor cells express Pax6 as early as
269 E11.5 (Fig. 8). Many *Zic4*-lineage postmitotic cells in the prethalamus retained Pax6 (e.g. yellow asterisks in
270 Fig. 8C); others did not (e.g. green asterisks in Fig. 8C). We went on to use the *Zic4^{Cre}* allele to test the
271 effects of mutating one or both copies of the *Pax6* gene in *Zic4*-lineage cells.

272 ***Zic4^{Cre}*-induced deletion of Pax6**

273 We studied Pax6 expression in *Zic4^{Cre};Pax6^{fl/+}* and *Zic4^{Cre};Pax6^{fl/fl}* embryos at E12.5, E13.5, E14.5 and E16.5.
274 For each genotype at each age, we examined three non-littermate embryos and the results were
275 indistinguishable. In *Zic4^{Cre};Pax6^{fl/fl}* homozygous mutant embryos (Fig. 4A3-F3,5A3-G3,6A3-G3,7A3-F3), the
276 numbers of cells immunostained for Pax6 declined rapidly in the thalamus from E12.5 onwards, particularly
277 in its anterior parts where many cells are *Zic4*-lineage. By E14.5, there were almost no Pax6-expressing
278 progenitors in the thalamus in *Zic4^{Cre};Pax6^{fl/fl}* embryos whereas normally a small population remained. The
279 numbers of Pax6-expressing cells in the prethalamus of *Zic4^{Cre};Pax6^{fl/fl}* embryos were greatly reduced at all
280 ages. There were no consistent defects in the overall shapes and sizes of diencephalic structures.

281 In *Zic4^{Cre};Pax6^{fl/+}* heterozygotes, we detected no defects of Pax6 expression at E12.5-E14.5 (Fig. 4A2-F2,5A2-
282 G2,6A2-G2). By E16.5, however, the numbers of Pax6-expressing cells had declined throughout the
283 prethalamus and the intensity of the immunostaining of many Pax6-expressing cells was lower than normal
284 (Fig. 7A2-F2). The pattern of Pax6 expression in *Zic4^{Cre};Pax6^{fl/+}* embryos now appeared intermediate
285 between controls and *Zic4^{Cre};Pax6^{fl/fl}* embryos. There were no detectable defects in the positions of the
286 Pax6-expressing cells. The overall shapes and sizes of diencephalic structures appeared normal. These
287 findings indicate that mutation of one copy of *Pax6* in *Zic4*-lineage cells causes them to lower their Pax6
288 levels between E14.5 and E16.5, i.e. once they are postmitotic neurons, with levels in some falling below
289 the threshold for detection.

290 **Cells of the vLGN, dLGN and the ventral posterior nuclei are generated before E14.5**

291 We selected three thalamic nuclei to search for defects resulting from mutation of *Pax6* in *Zic4*-lineage
292 cells: vLGN, which contains a large proportion of *Zic4*-lineage cells at birth; dLGN, which contains an
293 intermediate proportion of *Zic4*-lineage cells at birth; ventral posterior (VP) nuclei (VPM and VPL), which
294 contain low numbers of *Zic4*-lineage cells at birth.

295 As a first step towards testing whether *Pax6* mutation in *Zic4*-lineage cells affects the progenitors that give
296 rise to these nuclei, we checked the ages at which vLGN, dLGN and VP cells are generated. We injected
297 bromodeoxyuridine (BrdU) into control embryos at E10.5-E13.5 and studied BrdU labelling at birth (P0). To
298 help identify the nuclei we used several markers: COUP-TFI, COUP-TFII, LIM1/2 and Nkx2.2 (Fig. 9A-D).
299 COUP-TFI is expressed across most of the thalamic nuclei including the vLGN, dLGN and VP. The expression
300 level of COUP-TFI in the vLGN is lower than the surrounding nuclei such as the dLGN and VP and, within the
301 vLGN, is highest in the middle of the nucleus (Fig. 9A). COUP-TFII is expressed strongly in the prethalamus
302 and helped determine the anterior boundaries of the vLGN and VP (Fig. 9C). LIM1/2 and Nkx2.2 are strongly
303 expressed in the vLGN but not in the dLGN or VP (Fig. 9B,D).

304 We counted BrdU labelled cells as a proportion of all cells and as a proportion of *Zic4*-lineage (GFP+) cells in
305 each nucleus (Fig. 9E,F). We found that the vast majority of cells in vLGN, dLGN and VP are generated after
306 E10.5 and before E13.5 (Fig. 9G,H).

307 **Effects of *Pax6* mutation in *Zic4*-lineage cells on cell production**

308 We next used immunostaining for Ki67 (a marker of proliferating cells), Tuj1 (a marker of newly
309 differentiating neurons) and phosphohistone H3 (pHH3, a marker of cells in M-phase of the cell cycle)
310 together with short-term BrdU labelling to assess the activity of progenitors in regions that generate vLGN,
311 dLGN and VP at E11.5 and E12.5 (Fig. 10). We made measurements in three regions: pTH-C, which gives rise
312 to thalamic nuclei including dLGN and VP; pTH-R, which contributes to nuclei including vLGN; and
313 prethalamus (Fig. 10A). We sampled from four sections through each prethalamus and five through each
314 pTH-C and pTH-R, equally-spaced from anterior to posterior, from four embryos of each age and genotype.

315 We first made measurements on all cells in the three regions, i.e. including both GFP+ and GFP- cells. When
316 we examined the percentages of all cells that were proliferative based on their expression of Ki67, referred

317 to as the growth fraction, we found small but significant decreases in $Pax6^{fl/fl}$ pTH-C and pTH-R (Fig. 10B).
318 When we measured this same parameter specifically in GFP+ (*Zic4*-lineage) cells, we found no significant
319 effects of genotype (Fig. 10C). There were no inter-genotypic differences in the numbers of pHH3+ cells in
320 any region at either age (Fig. 10D,E). We then measured the proportions of proliferating cells (Ki67+) that
321 were in S-phase (BrdU+), which is an indication of their rate of proliferation (i.e. the longer the cell cycle,
322 the lower the proportion of cells in S-Phase within the defined time-window). When we examined all cells
323 we identified a small but significant decrease at E11.5 in $Pax6^{fl/fl}$ pTH-R (Fig. 10F). When we examined GFP+
324 cells alone, we found no significant effects of genotype (Fig. 10G).

325 These findings indicate that the loss of both copies of Pax6 in *Zic4*-lineage has a minor effect on
326 proliferation, causing decreases in pTH-C and/or pTH-R at some ages, which was only detectable in the
327 overall population of progenitors and not specifically the *Zic4*-lineage progenitors themselves.

328 ***Pax6* mutation in *Zic4*-lineage cells increases their contribution to vLGN and dLGN**

329 We then analysed the effects of *Pax6* mutation in *Zic4*-lineage cells on the numbers of these cells that
330 contribute to vLGN, dLGN and VP at P0 (Fig. 11). We first estimated the total numbers of cells in each of
331 these nuclei by sampling the densities of all counterstained cells in each nucleus and multiplying by its
332 volume. Volumes were estimated using the ImageJ Volumest plugin on a series of ten coronal sections with
333 a regular interval of 60 μ m from each brain sample. We found no significant inter-genotypic differences,
334 indicating that *Pax6* mutation in *Zic4*-lineage cells did not alter overall numbers of cells contributing to
335 these nuclei (Fig. 11D-F).

336 We measured the proportions of cells in each of these nuclei that were *Zic4*-lineage (i.e. GFP+). We found
337 that these proportions were significantly increased in the dLGN of $Pax6^{fl/fl}$ embryos (Fig. 11A,C,H). They
338 were increased even more in the dLGN of $Pax6^{fl/+}$ embryos, with more than twice the normal proportions of
339 *Zic4*-lineage cells contributing (Fig. 11A,B,H). Proportions were also increased in the vLGN of $Pax6^{fl/+}$
340 embryos (Fig. 11A,B,G). The increases in the dLGN were seen in anterior sections in $Pax6^{fl/fl}$ embryos and
341 throughout all sections in $Pax6^{fl/+}$ embryos (Fig. 11H). The increases in the vLGN in $Pax6^{fl/+}$ embryos were
342 greater in more posterior sections (Fig. 11G). There were no inter-genotypic differences in VP (Fig. 11I).

343 These findings indicate that the dLGN increases its content of *Zic4*-lineage cells at the expense of *Zic4*-non-
344 lineage cells if the *Zic4*-lineage cells are *Pax6*^{fl/fl} or *Pax6*^{fl/+}. The vLGN increases its content of *Zic4*-lineage
345 cells at the expense of *Zic4*-non-lineage cells if the *Zic4*-lineage cells are *Pax6*^{fl/+}.

346

347 **Discussion**

348 We have found that *Zic4*-lineage cells normally contribute ~50% of vLGN cells, ~25% of dLGN cells and ~10%
349 of VP cells at birth. Heterozygosity for a loss-of-function mutation of *Pax6* in *Zic4*-lineage cells greatly
350 increased the contribution that these cells make to the vLGN and dLGN, but not the VP. Homozygosity for
351 the same mutation had a smaller effect on the contribution of *Zic4*-lineage cells to the dLGN and no effect
352 on contribution to vLGN and VP.

353 These changes are most likely explained by a redistribution of mutant *Zic4*-lineage cells into the dLGN and
354 vLGN. Our findings argue against an alternative explanation involving overproduction of mutant *Zic4*-
355 lineage cells. When we tested whether *Pax6* mutation, either heterozygous or homozygous, had an effect
356 on the early proliferation of specifically the *Zic4*-lineage progenitors, we found none. We did find slight
357 decreases in proliferation in some regions at some ages when we considered the overall populations of
358 progenitors, both *Zic4*-lineage and *Zic4*-non-lineage. These finding suggest that some change in the *Zic4*-
359 lineage cells, perhaps involving altered signalling, had a cell non-autonomous effect on the *Zic4*-non-lineage
360 cells. It does not, however, provide a straightforward explanation for the increased numbers of mutant
361 *Zic4*-lineage cells in the dLGN and vLGN. Another reason that redistribution of postmitotic cells is a more
362 likely mechanism than altered production is that the effects of heterozygosity for *Pax6* mutation on Pax6
363 protein levels only became obvious in postmitotic cells and not in progenitors.

364 Figure 12 summarizes our model. The ZLI and the two progenitor domains posterior to it, pTH-R and pTH-C
365 (Fig. 12C,E), express substantially different sets of regulatory genes. For example, the ZLI expresses *Shh*,
366 pTH-R expresses transcription factors such as *Nkx2.2* and *Asc1*, and pTH-C expresses *Neurog1* and *Neurog2*.
367 Several previous fate mapping studies have used genetic tools to exploit these early gene expression
368 patterns to link specific sets of progenitors with mature diencephalic nuclei (Vue et al., 2007, 2009; Suzuki-

369 Hirano et al., 2011; Delauney et al., 2009; Jeong et al., 2011). These studies showed that the ZLI and
370 adjacent pTH-R contribute to the vLGN whereas more caudal progenitors in pTH-C contribute progressively
371 to more caudal thalamic nuclei. In other words, the relative positions of thalamic progenitors are well
372 preserved in the spatial arrangement of the nuclei they generate. Pax6 is expressed in a gradient by
373 thalamic progenitors, with its lowest levels in pTH-R and no expression in the ZLI (Fig. 12C,E). This means
374 that the *Zic4*-lineage cells that distribute to the vLGN and dLGN are derived mainly from progenitors that
375 express little or no Pax6. If homozygous or heterozygous mutation causes *Zic4*-lineage cells to lose or lower
376 their levels of Pax6, then these cells or their daughters preferentially distribute to nuclei that are generated
377 from progenitors that express little or no Pax6. This suggests that the positional information encoded by
378 the levels of Pax6 in diencephalic progenitors is an important determinant of the eventual locations of their
379 daughter cells.

380 A likely mechanism by which Pax6 levels effect the distribution of diencephalic neurons is through its
381 regulation of cell adhesion molecules that cause cells to sort on the basis of their intercellular interactions.
382 It has long been appreciated in many different systems that cells aggregate if they have similar levels of
383 cadherins (Foty and Steinberg, 2005; Halbleib and Nelson, 2006). In the postnatal mouse brain, different
384 thalamic nuclei express distinct combinations of cadherins: for example, the vLGN and dLGN express
385 Cadherin 5, 8 and 11 whereas VP expresses mainly Cadherin 6 and 11 (Suzuki et al., 1997; Hirano and
386 Takeichi, 2012). Both *in vivo* and *in vitro* studies have shown that Pax6 can regulate molecules such as R-
387 cadherin, L1 cell adhesion molecule and N-CAM (Andrews and Mastick, 2003; Tyas et al., 2003; Meech et
388 al., 1999; Stoykova et al., 1997; Holst et al., 1997; Edelman and Jones, 1995; Chalepakis et al., 1994).

389 Why *Zic4*-lineage cells heterozygous for a mutation of *Pax6* cause a greater redistribution of *Zic4*-lineage
390 cells affecting both dLGN and vLGN is not clear. One possibility stems from our observation that
391 heterozygosity has a relatively late effect on Pax6 levels in postmitotic neurons, which contribute mainly to
392 the prethalamus. A reduction of Pax6 levels in migrating prethalamus might allow significant
393 numbers of these cells to migrate in an abnormal direction across the boundary from prethalamus into the
394 vLGN and dLGN. The numbers that do this might be greater than the numbers that sort incorrectly

395 following loss of Pax6 from progenitors, as occurs in homozygous deletion. Progenitors might possess a
396 degree of plasticity that allows them to compensate to some degree if they lose Pax6, thereby minimizing
397 the consequences for later sorting of their postmitotic cells.

398 Whatever the cause of the strong effect of Pax6 heterozygosity, this finding is particularly relevant to
399 human disease caused by *PAX6* haploinsufficiency. In humans, heterozygous loss-of-function mutations
400 affecting *PAX6* cause a disorder with an incidence of ~1/50,000 live births. Patients show a range of
401 neurological and psychiatric symptoms including impaired auditory processing, verbal function and social
402 cognition, autism and mental retardation and altered functional connectivity in intrinsic neural networks
403 (Sisodiya et al., 2001; Free et al., 2003; Mitchell et al., 2003; Bamiou et al., 2007; Umeda et al., 2010;
404 Ellison-Wright et al., 2004; Thompson et al., 2004; Pierce et al., 2014). These functional abnormalities are
405 associated with structural defects of the cerebral cortex and its axonal tracts (Sisodiya et al., 2001). Mice
406 with heterozygous loss-of-function mutations of *Pax6* have rarely been used to explore possible
407 pathologies underlying the neurological and psychiatric symptoms that patients experience. Although one
408 study suggested a slight delay in the onset of corticogenesis in *Pax6*^{+/-} embryos (Schmahl et al., 1993), other
409 work found no abnormalities of cortical development in these mice (Mi et al., 2013). Almost nothing is
410 reported on the effects of *Pax6*^{+/-} heterozygosity on development of the diencephalon. Given that the dLGN
411 is the relay nucleus for projections to the visual cortex, the findings of this study suggest that defects of the
412 thalamus and geniculocortical pathway might be found in patients.

413 **References**

- 414 Andrews GL, Mastick GS (2003) R-cadherin is a Pax6-regulated, growth-promoting cue for pioneer axons. *J*
415 *Neurosci* 23:9873-9880.
- 416 Aruga J, Nagai T, Tokuyama T, Hayashizaki Y, Okazaki Y, Chapman VM, Mikoshiba K (1996) The mouse zic
417 gene family. Homologues of the *Drosophila* pair-rule gene odd-paired. *J Biol Chem* 271:1043-1047.
- 418 Aruga J, Yozu A, Hayashizaki Y, Okazaki Y, Chapman VM, Mikoshiba K (1996) Identification and
419 characterization of Zic4, a new member of the mouse Zic gene family. *Gene* 172:291-294.
- 420 Bamiou DE, Free SL, Sisodiya SM, Chong WK, Musiek F, Williamson KA, van Heyningen V, Moore AT, Gadian
421 D, Luxon LM (2007) Auditory interhemispheric transfer deficits, hearing difficulties, and brain magnetic
422 resonance imaging abnormalities in children with congenital aniridia due to PAX6 mutations. *Arch Pediatr*
423 *Adolesc Med* 161:463–469.
- 424 Caballero IM, Manuel MN, Molinek M, Quintana-Urzaiz I, Mi D, Shimogori T, Price DJ (2014) Cell-
425 autonomous repression of Shh by transcription factor Pax6 regulates diencephalic patterning by controlling
426 the central diencephalic organizer. *Cell Rep* 8: 1405-1418.
- 427 Chalepakis G, Wijnholds J, Giese P, Schachner M, Gruss P (1994) Characterization of Pax-6 and Hoxa-1
428 binding to the promoter region of the neural cell adhesion molecule L1. *DNA Cell Biol* 13:891-900.
- 429 Delaunay D, Heydon K, Miguez A, Schwab M, Nave KA, Thomas JL, Spassky N, Martinez S, Zalc B (2009)
430 Genetic tracing of subpopulation neurons in the prethalamus of mice (*Mus musculus*). *J Comp Neurol*
431 512:74-83.
- 432 Edelman GM, Jones FS (1995) Developmental control of N-CAM expression by Hox and Pax gene products.
433 *Philos Trans R Soc Lond B Biol Sci* 349:305-312.
- 434 Ellison-Wright Z, Heyman I, Frampton I, Rubia K, Chitnis X, Ellison-Wright I, Williams SC, Suckling J, Simmons
435 A, Bullmore E (2004) Heterozygous PAX6 mutation, adult brain structure and fronto-striato-thalamic
436 function in a human family. *Eur J Neurosci* 19:1505–1512.

- 437 Ericson J, Rashbass P, Schedl A, Brenner-Morton S, Kawakami A, van Heyningen V, Jessell TM, Briscoe J
438 (1997) Pax6 controls progenitor cell identity and neuronal fate in response to graded Shh signaling. *Cell*
439 90:169-180.
- 440 Foty RA, Steinberg MS (2005) The differential adhesion hypothesis: a direct evaluation. *Dev Biol* 278:255-
441 263.
- 442 Free SL, Mitchell TN, Williamson KA, Churchill AJ, Shorvon SD, Moore AT, van Heyningen V, Sisodiya SM
443 (2003) Quantitative MR image analysis in subjects with defects in the PAX6 gene. *Neuroimage* 20: 2281-
444 2290.
- 445 Gaston-Massuet C, Henderson DJ, Greene ND, Copp AJ (2005) Zic4, a zinc-finger transcription factor, is
446 expressed in the developing mouse nervous system. *Dev Dyn* 233:1110-1115.
- 447 Halbleib JM, Nelson WJ (2006) Cadherins in development: cell adhesion, sorting, and tissue morphogenesis.
448 *Genes Dev* 20:3199-3124.
- 449 Hirano S, Takeichi M. (2012) Cadherins in brain morphogenesis and wiring. *Physiol Rev.* 92:597-634.
- 450 Holst BD, Wang Y, Jones FS, Edelman GM (1997) A binding site for Pax proteins regulates expression of the
451 gene for the neural cell adhesion molecule in the embryonic spinal cord. *Proc Natl Acad Sci U S A* 94:1465-
452 70.
- 453 Horng S, Kreiman G, Ellsworth C, Page D, Blank M, Millen K, Sur M (2009) Differential gene expression in the
454 developing lateral geniculate nucleus and medial geniculate nucleus reveals novel roles for Zic4 and Foxp2
455 in visual and auditory pathway development. *J Neurosci* 29:13672-13683.
- 456 Jeong Y, Dolson DK, Waclaw RR, Matisse MP, Sussel L, Campbell K, Kaestner KH, Epstein DJ (2011) Spatial
457 and temporal requirements for sonic hedgehog in the regulation of thalamic interneuron identity.
458 *Development* 138:531-541.
- 459 Jones E (2007) *The thalamus*. Cambridge: Cambridge University Press.
- 460 Lamprecht MR, Sabatini DM, Carpenter AE (2007) CellProfiler: free, versatile software for automated
461 biological image analysis. *Biotechniques* 42:71-75.

- 462 Lim Y and Golden J (2007) Patterning the developing diencephalon. *Brain Res Rev* 53:17-26.
- 463 Macdonald R, Barth KA, Xu Q, Holder N, Mikkola I, Wilson SW (1995) Midline signalling is required for Pax
464 gene regulation and patterning of the eyes. *Development* 121:3267-3278.
- 465 Martinez-Ferre A and Martinez S (2012) Molecular Regionalization of the Diencephalon. *Frontiers in*
466 *Neuroscience* 6.
- 467 Martynoga B, Morrison H, Price DJ, Mason JO. (2005) *Foxg1* is required for specification of ventral
468 telencephalon and region-specific regulation of dorsal telencephalic precursor proliferation and apoptosis.
469 *Dev Biol.* 283:113-27.
- 470 Meech R, Kallunki P, Edelman GM, Jones FS (1999) A binding site for homeodomain and Pax proteins is
471 necessary for L1 cell adhesion molecule gene expression by Pax-6 and bone morphogenetic proteins. *Proc*
472 *Natl Acad Sci U S A* 96:2420-2425.
- 473 Merzin M (2008) Applying stereological method in radiology. Volume measurement. Bachelor's thesis.
474 University of Tartu.
- 475 Mi D, Carr CB, Georgala PA, Huang YT, Manuel MN, Jeanes E, Niisato E, Sansom SN, Livesey FJ, Theil T,
476 Hasenpusch-Theil K, Simpson TI, Mason JO, Price DJ (2013) Pax6 exerts regional control of cortical
477 progenitor proliferation via direct repression of Cdk6 and hypophosphorylation of pRb. *Neuron* 78:269-284.
- 478 Mitchell TN, Free SL, Williamson KA, Stevens JM, Churchill AJ, Hanson IM, Shorvon SD, Moore AT, van
479 Heyningen V, Sisodiya SM (2003) Polymicrogyria and absence of pineal gland due to PAX6 mutation. *Ann*
480 *Neurol* 53:658–663.
- 481 Miyoshi G, Hjerling-Leffler J, Karayannis T, Sousa VH, Butt SJ, Battiste J, Johnson JE, Machold RP, Fishell G
482 (2010) Genetic fate mapping reveals that the caudal ganglionic eminence produces a large and diverse
483 population of superficial cortical interneurons. *J Neurosci* 30:1582-1594.
- 484 Nakagawa Y, Shimogori T (2012) Diversity of thalamic progenitor cells and postmitotic neurons. *Eur J*
485 *Neurosci* 35:1554-1562.

- 486 Pierce JE, Krafft CE, Rodrigue AL, Bobilev AM, Lauderdale JD, McDowell JE (2014) Increased functional
487 connectivity in intrinsic neural networks in individuals with aniridia. *Front Hum Neurosci* 8:01013.
- 488 Robertshaw E1, Matsumoto K, Lumsden A, Kiecker C (2013) *Irx3* and *Pax6* establish differential competence
489 for Shh-mediated induction of GABAergic and glutamatergic neurons of the thalamus. *Proc Natl Acad Sci U*
490 *S A* 110:3919-3926.
- 491 Rubin AN, Alfonsi F, Humphreys MP, Choi CK, Rocha SF, Kessar N (2010) The germinal zones of the basal
492 ganglia but not the septum generate GABAergic interneurons for the cortex. *J Neurosci* 30:12050-12062.
- 493 Schmahl W, Knoedlseder M, Favor J, Davidson D (1993) Defects of neuronal migration and the pathogenesis
494 of cortical malformations are associated with Small eye (*Sey*) in the mouse, a point mutation at the *Pax-6*-
495 locus. *Acta Neuropathol* 86:126-135.
- 496 Sherman S and Guillery R (2002) The role of the thalamus in the flow of information to the cortex. *Philos*
497 *Trans R Soc Lond B Biol Sci* 357:1695-1708.
- 498 Sherman S and Guillery R (2006) Exploring the thalamus and its role in cortical function. Cambridge,
499 Massachusetts: MIT Press.
- 500 Sherman S and Guillery R (2011) Distinct functions for direct and transthalamic corticocortical connections.
501 *Journal of Neurophysiology* 106:1068-1077.
- 502 Simpson TI, Pratt T, Mason JO, Price DJ (2009) Normal ventral telencephalic expression of *Pax6* is required
503 for normal development of thalamocortical axons in embryonic mice. *Neural Dev* 4:19.
- 504 Sisodiya SM, Free SL, Williamson KA, Mitchell TN, Willis C, Stevens JM, Kendall BE, Shorvon SD, Hanson IM,
505 Moore AT, van Heyningen V (2001) *PAX6* haploinsufficiency causes cerebral malformation and olfactory
506 dysfunction in humans. *Nat Genet* 28:214–216.
- 507 Stoykova A, Götz M, Gruss P, Price J (1997) *Pax6*-dependent regulation of adhesive patterning, R-cadherin
508 expression and boundary formation in developing forebrain. *Development* 124:3765-3777.
- 509 Suzuki SC, Inoue T, Kimura Y, Tanaka T, Takeichi M. (1997) Neuronal circuits are subdivided by differential
510 expression of type-II classic cadherins in postnatal mouse brains. *Mol Cell Neurosci*. 9:433-47.

- 511 Suzuki-Hirano A, Ogawa M, Kataoka A, Yoshida AC, Itoh D, Ueno M, Blackshaw S, Shimogori T (2011)
512 Dynamic spatiotemporal gene expression in embryonic mouse thalamus. *J Comp Neurol* 519:528-543.
- 513 Thompson PJ, Mitchell TN, Free SL, Williamson KA, Hanson IM, van Heyningen V, Moore AT, Sisodiya SM
514 (2004) Cognitive functioning in humans with mutations of the PAX6 gene. *Neurology* 62:1216 –1218.
- 515 Tyas DA, Pearson H, Rashbass P, Price DJ (2003) Pax6 regulates cell adhesion during cortical development.
516 *Cereb Cortex* 13:612-619.
- 517 Umeda T, Takashima N, Nakagawa R, Maekawa M, Ikegami S, Yoshikawa T, Kobayashi K, Okanoya K,
518 Inokuchi K, Osumi N (2010) Evaluation of Pax6 mutant rat as a model for autism. *PLoS One* 5:e15500.
- 519 Vue TY, Aaker J, Taniguchi A, Kazemzadeh C, Skidmore JM, Martin DM, Martin JF, Treier M, Nakagawa Y
520 (2007) Characterization of progenitor domains in the developing mouse thalamus. *J Comp Neurol* 505:73-
521 91.
- 522 Vue TY, Bluske K, Alishahi A, Yang LL, Koyano-Nakagawa N, Novitch B, Nakagawa Y (2009) Sonic hedgehog
523 signaling controls thalamic progenitor identity and nuclei specification in mice. *J Neurosci* 29:4484-4497.

524 **Figure legends**

525

526 **Figure 1. Expression of *Zic4* and activity of *Zic4*^{Cre} in *Zic4*^{Cre+/-};*RCE*^{+/-} mouse brain coronal sections at E11.5**

527 **and E12.5.** (A,G) Schematics of E11.5 and E12.5 mouse brain demarcating major subdivisions and sectioning

528 planes. (B1-F,H1-J3) *Zic4* fluorescent in situ hybridisation (monochrome in B1,C1,D1,H1,I1,J1 or red in

529 B3,C3,D3,E,F,H3,I3,J3) and immunohistochemistry for GFP reporter of *Zic4*^{Cre} activity (monochrome in

530 B2,C2,D2,H2,I2,J2 or green in B3,C3,D3,E,F,H3,I3,J3) with DAPI counterstaining (blue). Box in D3 is shown in

531 E; box in E is shown in F. Scale bars: B1-D3,H1-J3, 250 μ m; E, 125 μ m; F, 25 μ m. Cx, cortex; cp, choroid

532 plexus; MGE, medial ganglionic eminence; LGE, lateral ganglionic eminence; th, thalamus; pth,

533 prethalamus; emt, eminentia thalami; epi, epithalamus.

534

535 **Figure 2. Expression of *Zic4* and activity of *Zic4*^{Cre} in *Zic4*^{Cre+/-};*RCE*^{+/-} mouse brain coronal sections at E13.5,**

536 **E14.5 and E15.5.** (A,E,I) Schematics of E13.5, E14.5 and E15.5 mouse brain demarcating major subdivisions

537 and sectioning planes. (B1-D3,F1-H3,J1-L3) *Zic4* fluorescent in situ hybridisation (monochrome in

538 B1,C1,D1,F1,G1,H1,J1,K1,L1 or red in B3,C3,D3,F3,G3,H3, J3,K3,L3) and immunohistochemistry for GFP

539 reporter of *Zic4*^{Cre} activity (monochrome in B2,C2,D2,F2,G2,H2,J2,K2,L2 or green in B3,C3,D3,F3,G3,H3,

540 J3,K3,L3) with DAPI counterstaining (blue). Scale bars: 250 μ m. vLGN, ventral lateral geniculate nucleus; th,

541 thalamus; pth, prethalamus.

542

543 **Figure 3. Expression of *Zic4* and activity of *Zic4*^{Cre} in *Zic4*^{Cre+/-};*RCE*^{+/-} mouse brain coronal sections at E16.5,**

544 **E18.5 and postnatal day (P) 0.** (A,E,H) Schematics of E16.5, E18.5 and P0 mouse brain demarcating major

545 subdivisions and nuclei and sectioning planes. (B1-D3,F1-G3) *Zic4* fluorescent in situ hybridisation

546 (monochrome in B1,C1,D1,F1,G1 or red in B3,C3,D3,F3,G3) and immunohistochemistry for GFP reporter of

547 *Zic4*^{Cre} activity (monochrome in B2,C2,D2,F2,G2 or green in B3,C3,D3,F3,G3,I) with DAPI counterstaining

548 (blue). Scale bars: B1-G3, 250 μ m; I, 500 μ m. Cx, cortex; dLGN, dorsal lateral geniculate nucleus; Hippo,

549 hippocampus; LD, lateral dorsal nucleus; LH, lateral habenula; LP, lateral posterior nucleus; MD, medial

550 dorsal nucleus; MH, medial habenula; PO, posterior nucleus; pth, prethalamus; PV, paraventricular nucleus;
551 RE, nucleus reunions; RH, rhomboid nucleus; SPF, subparafascicular thalamic nucleus; th, thalamus; VAL,
552 ventral anterolateral nucleus; vLGN, ventral lateral geniculate nucleus; VM, ventromedial nucleus; VPL,
553 ventral posterolateral nucleus; VPM = ventral posteromedial nucleus; vTel, ventral telencephalon; ZI, zona
554 incerta. (H) Adapted from Allen Brain Atlas <http://developingmouse.brain-map.org/>.

555

556 **Figure 4. Pax6 expression in control and Pax6 mutant embryos at E12.5.** Immunohistochemistry for Pax6
557 on a set of sections cut through the diencephalon in similar planes of section to those shown in Figure 1.
558 Boxed areas in B1-3 are enlarged in F1-3. ZLI, zona limitans intrathalamica; epi, epithalamus; th, thalamus;
559 pth, prethalamus; emt, eminentia thalami; h, hypothalamus. Scale bars, A1-E3, 500 μm ; F1-3, 50 μm .

560

561 **Figure 5. Pax6 expression in control and Pax6 mutant embryos at E13.5.** Immunohistochemistry for Pax6
562 on a set of sections cut through the diencephalon in similar planes of section to those shown in Figure 2.
563 Boxed areas in A1-B3 are enlarged in F1-G3. vLGN, ventral lateral geniculate nucleus; epi, epithalamus; th,
564 thalamus; pth, prethalamus; emt, eminentia thalami; h, hypothalamus. Scale bars, A1-E3, 500 μm ; F1-3, 50
565 μm .

566

567 **Figure 6. Pax6 expression in control and Pax6 mutant embryos at E14.5.** Immunohistochemistry for Pax6
568 on a set of sections cut through the diencephalon in similar planes of section to those shown in Figure 2. ZI,
569 zona incerta; vLGN, ventral lateral geniculate nucleus; th, thalamus; pth, prethalamus; emt, eminentia
570 thalami. Scale bar, 500 μm .

571

572 **Figure 7. Pax6 expression in control and Pax6 mutant embryos at E16.5.** Immunohistochemistry for Pax6
573 on a set of sections cut through the diencephalon in similar planes of section to those shown in Figure 3. ZI,
574 zona incerta; vLGN, ventral lateral geniculate nucleus; th, thalamus; pth, prethalamus. Scale bar, 500 μm .

575

576 **Figure 8. Diencephalic *Zic4*-lineage cells express *Pax6*.** Double-immunohistochemistry for GFP (*Zic4*-lineage
577 cells) and *Pax6* at E11.5. Area outlined in B is enlarged in C. Asterisks in C: yellow, examples of double-
578 labelled cells; green, examples of cells labelled only with GFP. Scale bars: A, 250 μm ; B, 50 μm ; C, 10 μm .

579

580 **Figure 9. Birthdates of cells in the vLGN, dLGN and VP.** (A-D) Immunohistochemistry at P0 with markers
581 designed to help delineate borders of the thalamic nuclei analysed here. Scale bar, 100 μm . (E,F) Example of
582 BrdU and GFP immunohistochemistry in vLGN. Scale bars, E, 100 μm ; F, 10 μm . (G) Proportions of all cells in
583 each nucleus that were BrdU+ after injection with BrdU at E10.5-13.5. (H) Proportions of GFP-expressing
584 cells in each nucleus that were BrdU+ after injection with BrdU at E10.5-13.5. Data points are from
585 individual animals. Means \pm sem are shown in each case. One-way ANOVA returned significant effects of
586 age in all cases: (G) vLGN $F(3,12)=7.729$, $P=0.0039$; dLGN $F(3,12)=13.56$, $P=0.0004$; VP $F(3,12)=20.76$,
587 $P<0.0001$. (H) vLGN $F(3,12)=8.282$, $P=0.0030$; dLGN $F(3,12)=15.41$, $P=0.0002$; VP $F(3,12)=23.26$, $P<0.0001$.
588 Holm-Sidak's multiple comparisons tests were performed following one-way ANOVA: * $P < 0.05$; ** $P < 0.01$;
589 *** $P < 0.001$; **** $P < 0.0001$.

590

591 **Figure 10. Effects of *Pax6* mutation in *Zic4*-lineage cells on early diencephalic progenitor proliferation.** (A)
592 Triple immunostaining for Tuj1, Ki67 and GFP. Three regions of interest were selected for analysis, one
593 midway through pTH-C, one in pTH-R and one in prethalamus (pth). Scale bars, 50 μm . (B) Average growth
594 fractions (\pm sem) in five equally spaced sections through pTH-C and pTH-R and four through prethalamus at
595 E11.5 and E12.5; colour coding for genotypes as in E. Two-way ANOVA detected significant effects of
596 genotype only in pTH-C ($F(2,30)=9.109$, $P=0.0008$) and pTH-R ($F(2,30)=11.97$, $P=0.0002$) at E12.5 ($n = 3$
597 embryos of each genotype), with *Pax6*^{f/f} embryos showing lower growth fractions at all levels (post hoc
598 Tukey's multiple comparisons test, $P<0.01$ at all positions). (C) Average growth fraction for GFP+ cells only.
599 There were no significant effects of genotype. (D) An example of triple immunostaining for pHH3, BrdU and
600 GFP in one region of interest. (E) Mean (\pm sem) counts of the total numbers of pHH3+ cells in all sampling

601 regions from each domain for each genotype. There were no significant effects of genotype. (F) Average
602 proliferation rates (\pm sem) in five equally spaced sections through pTH-C and pTH-R and four through
603 prethalamus at E11.5 and E12.5; colour coding for genotypes as in E. Two-way ANOVA showed a significant
604 effect of genotype in pTH-R at E11.5 ($F(2,30)=4.206$, $P=0.0245$), with lower values in $Pax6^{fl/+}$ embryos than
605 in the other two genotypes. (G) Average proliferation rates for GFP+ cells only. There were no significant
606 effects of genotype.

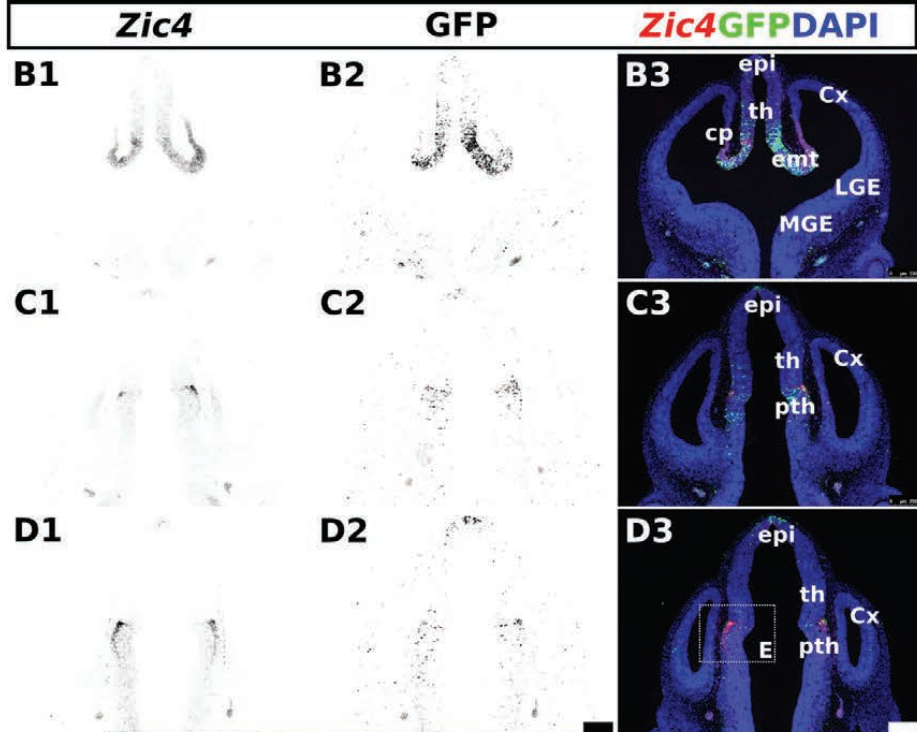
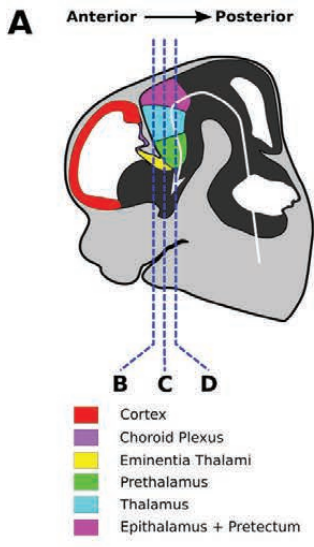
607

608 **Figure 11. Pax6 mutation in Zic4-lineage cells increases their contribution to vLGN and dLGN.** (A-C)
609 Sections from rostral to caudal through the diencephalon of P0 $Zic4^{Cre};Pax6^{+/+}$, $Zic4^{Cre};Pax6^{fl/+}$ and
610 $Zic4^{Cre};Pax6^{fl/fl}$ embryos. Scale bar 750 μ m. (D-F) Total numbers of cells in vLGN, dLGN and VP in four P0
611 pups of each genotype; individual values, means \pm sem are shown. There were no significant effects of
612 genotype. (G-I) Proportions of GFP+ (i.e. *Zic4*-lineage) cells in sections equally spaced through the vLGN,
613 dLGN and VP of P0 $Zic4^{Cre};Pax6^{+/+}$, $Zic4^{Cre};Pax6^{fl/+}$ and $Zic4^{Cre};Pax6^{fl/fl}$ pups. In vLGN and dLGN, two-way
614 ANOVA showed significant effects of genotype: vLGN, $F(2,90)=23.98$, $P<0.0001$; dLGN, $F(2,60)=140.4$,
615 $P<0.0001$. In VP, there were no significant effects. Data are plotted using means and sems using at least
616 three pups of each genotype ($n = 4$ for vLGN and $n = 3$ for dLGN and VP).

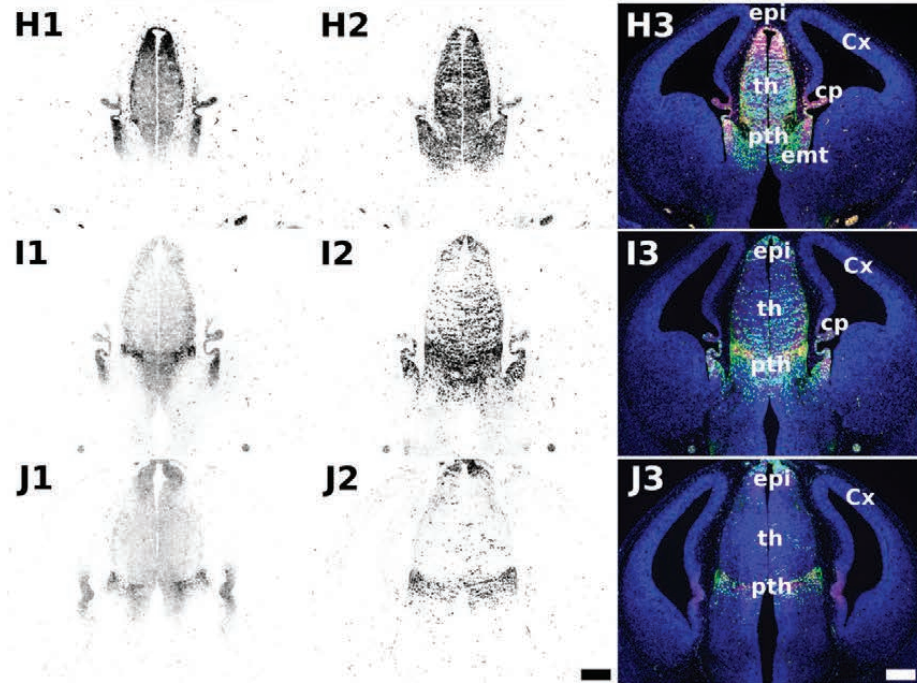
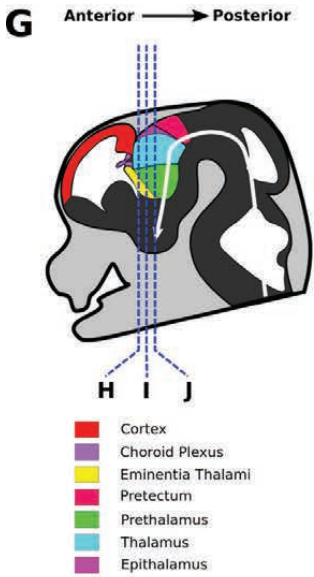
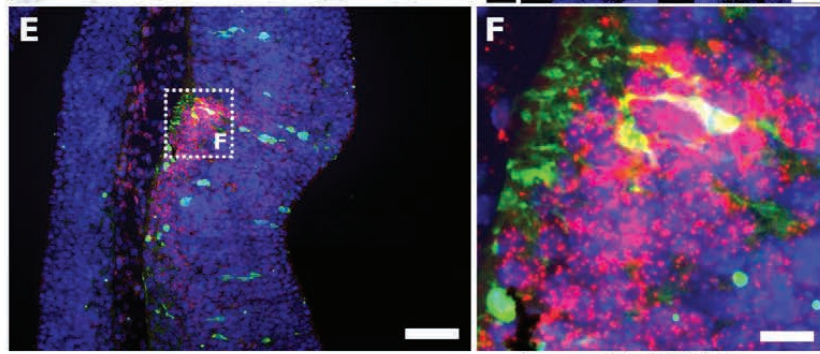
617

618 **Figure 12. Model.** (A,B) Sections through the embryonic thalamus (th) and prethalamus (pth) showing the
619 locations of the zona limitans intrathalamica (ZLI; red) and pTH-R (dark blue). (C,D) Normally, *Zic4*-lineage
620 cells from progenitors in the ZLI and pTH-R, which express little or no Pax6, contribute to the vLGN. *Zic4*-
621 lineage cells from progenitors in rostral pTH-C (i.e. close to pTH-R), whose levels of Pax6 are relatively low,
622 contribute to dLGN. *Zic4*-lineage cells in prethalamus (pth), which express Pax6 at high levels in both
623 progenitors and postmitotic neurons, contribute to prethalamic regions including the zona incerta (ZI). (E,F)
624 Mutant *Zic4*-lineage cells concentrate in the vLGN and/or dLGN, which are derived from thalamic
625 progenitors that normally express little or no Pax6.

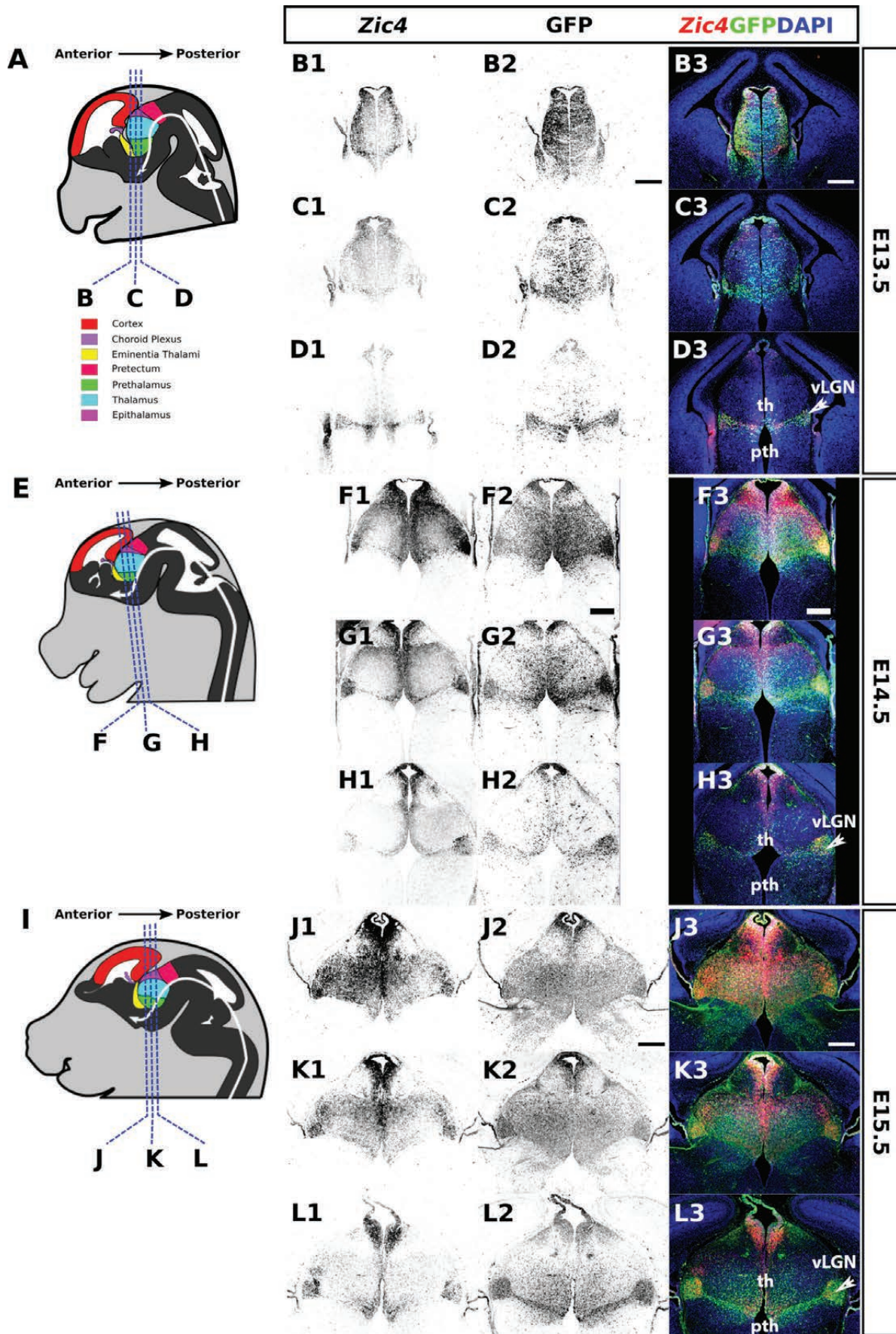
626

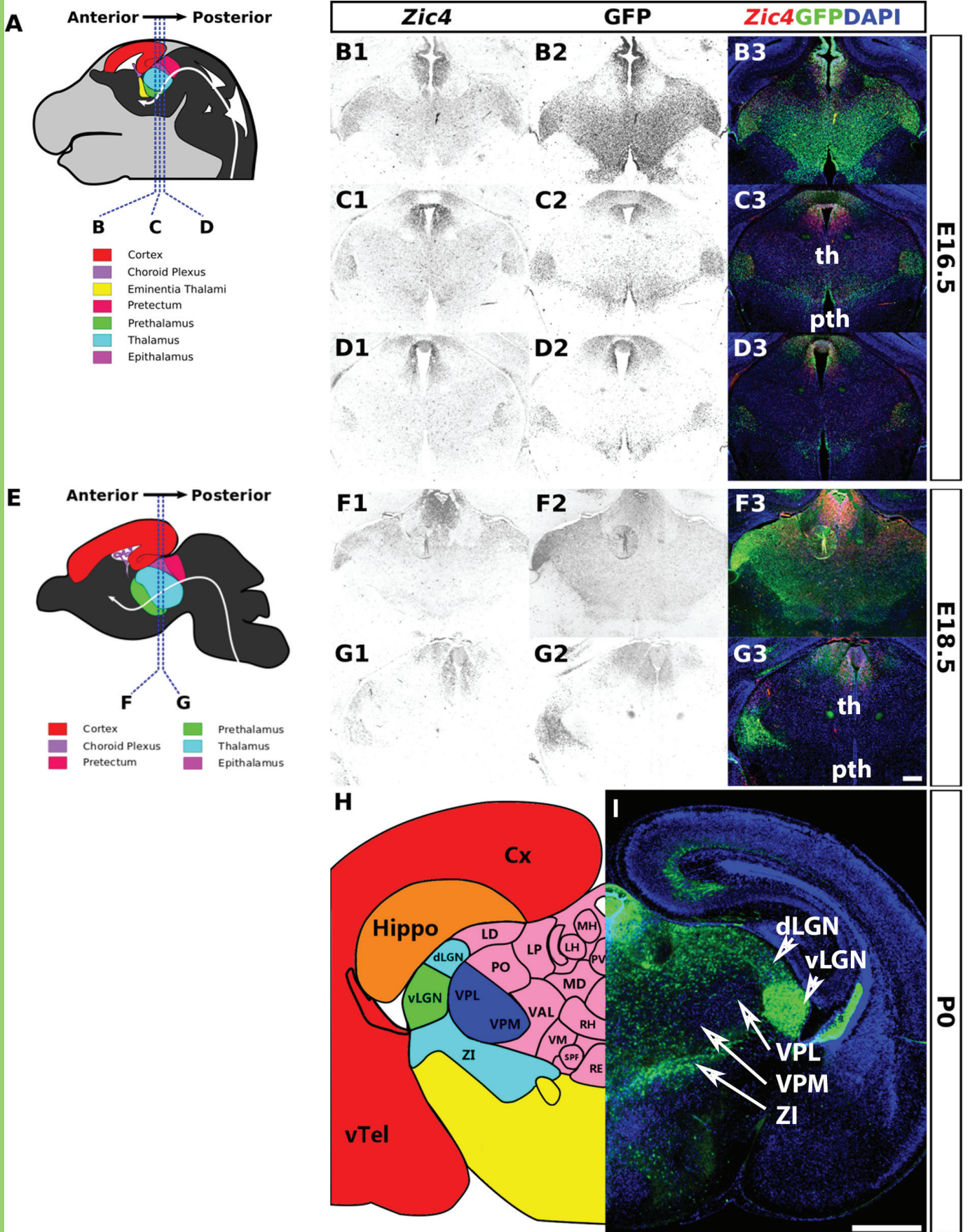


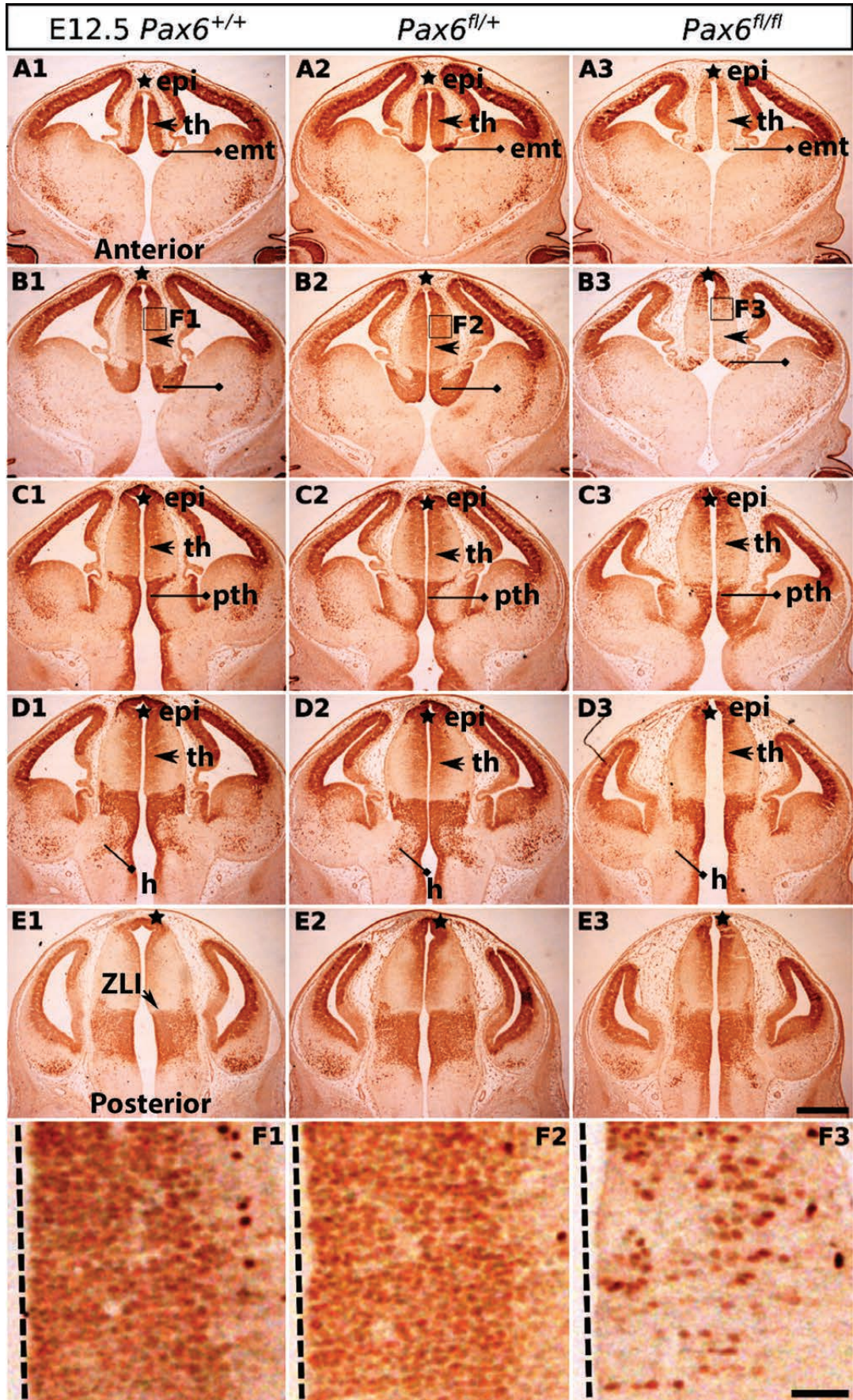
E11.5

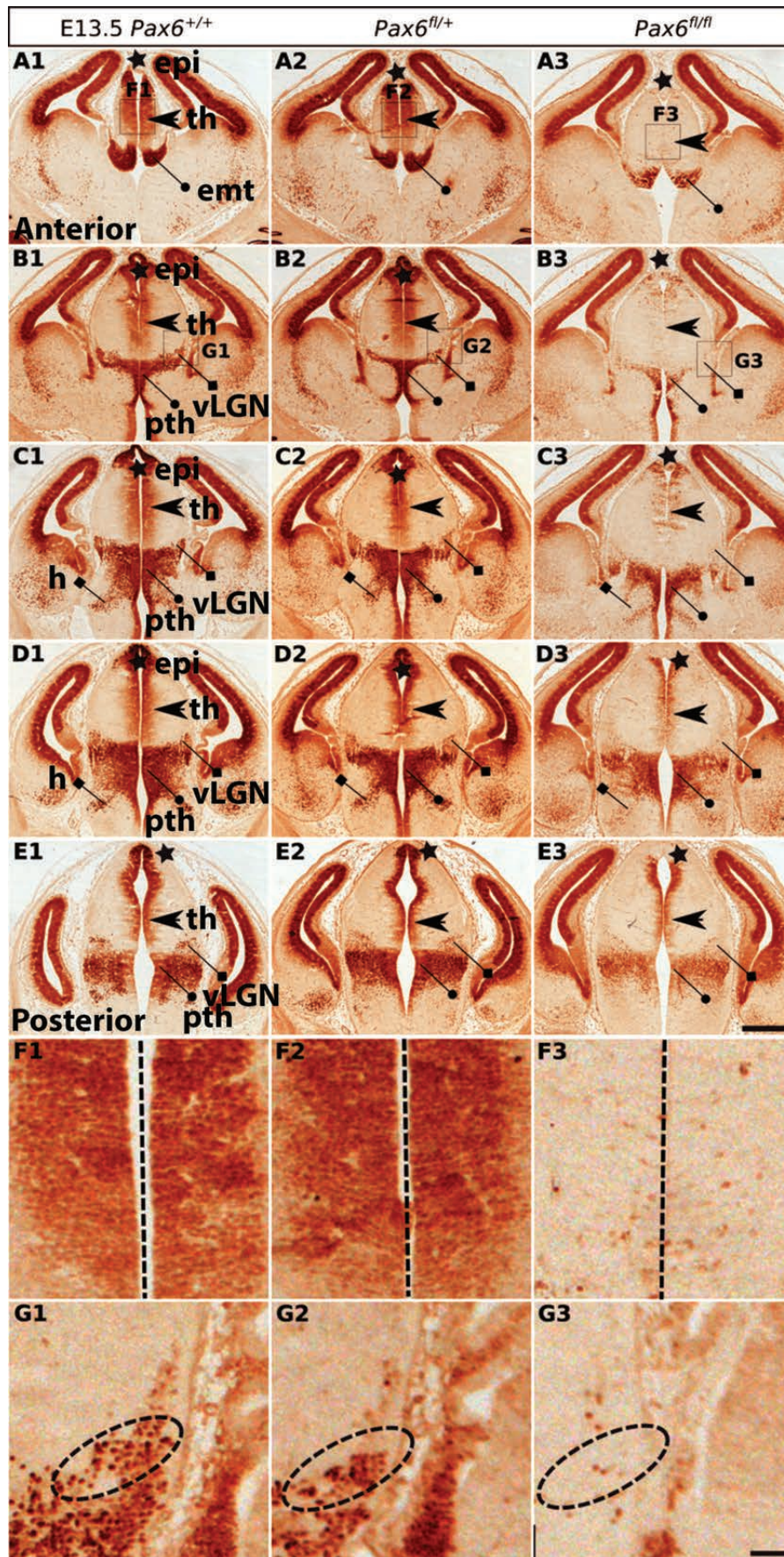


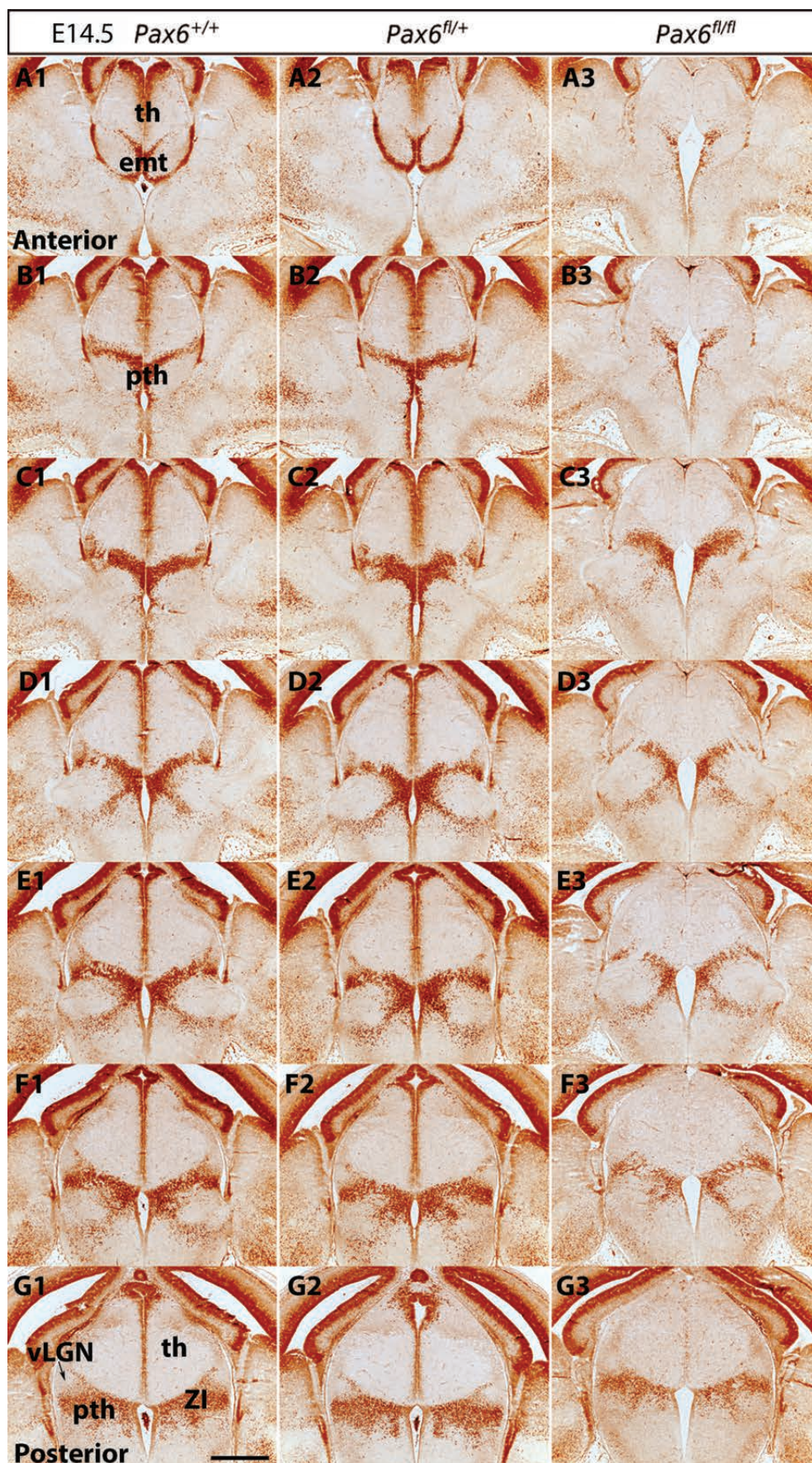
E12.5

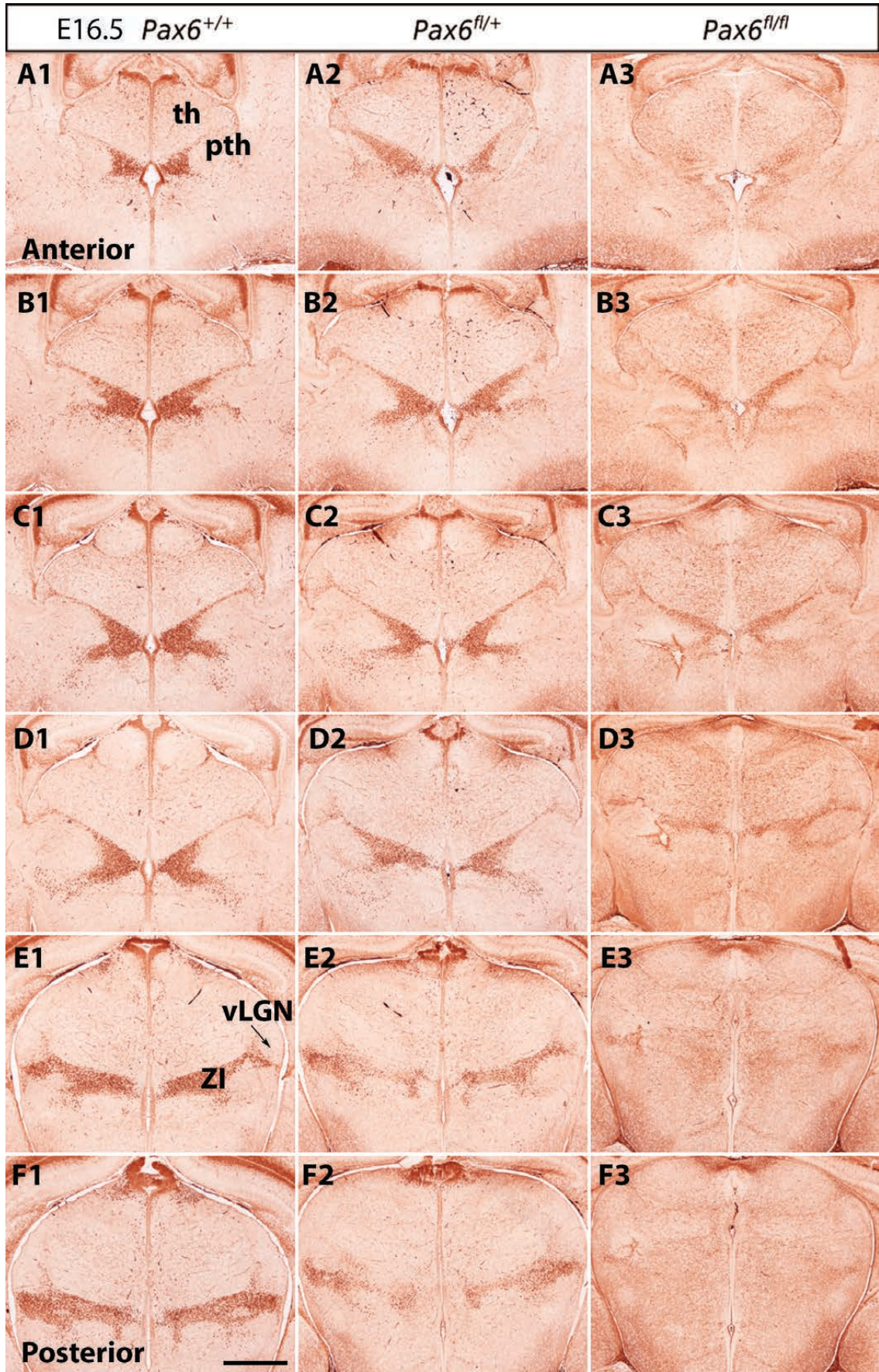


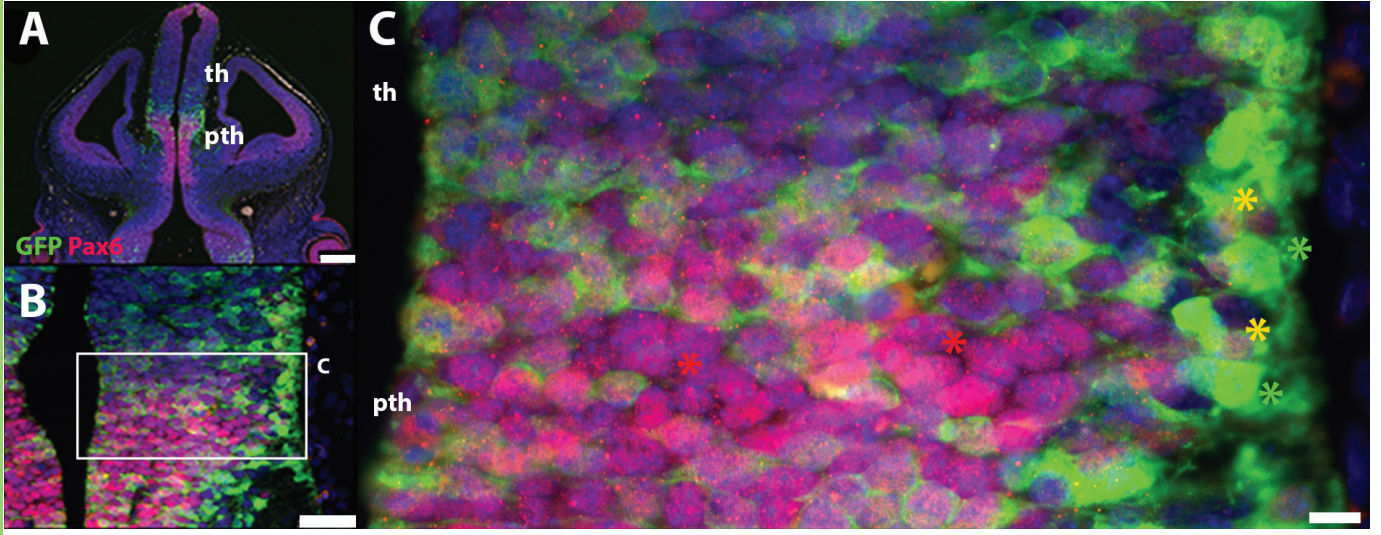


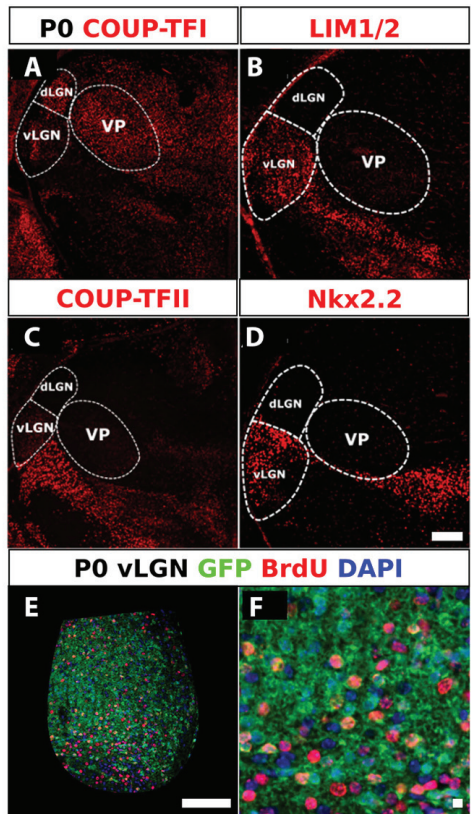




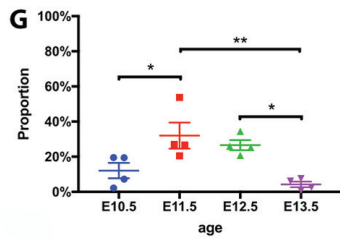




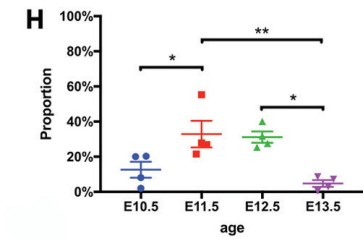




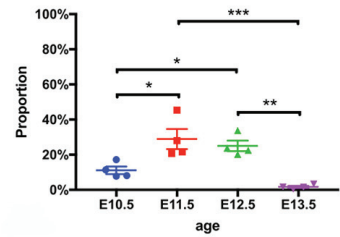
Proportion of vLGN cells born at different ages



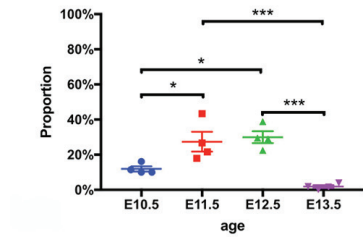
Proportion of GFP+ve vLGN cells born at different ages



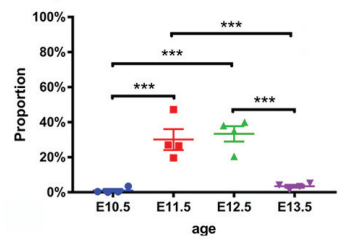
Proportion of dLGN cells born at different ages



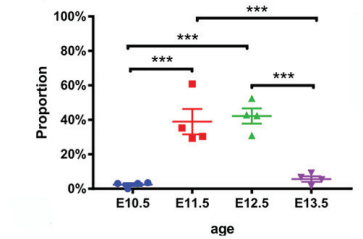
Proportion of GFP+ve dLGN cells born at different ages

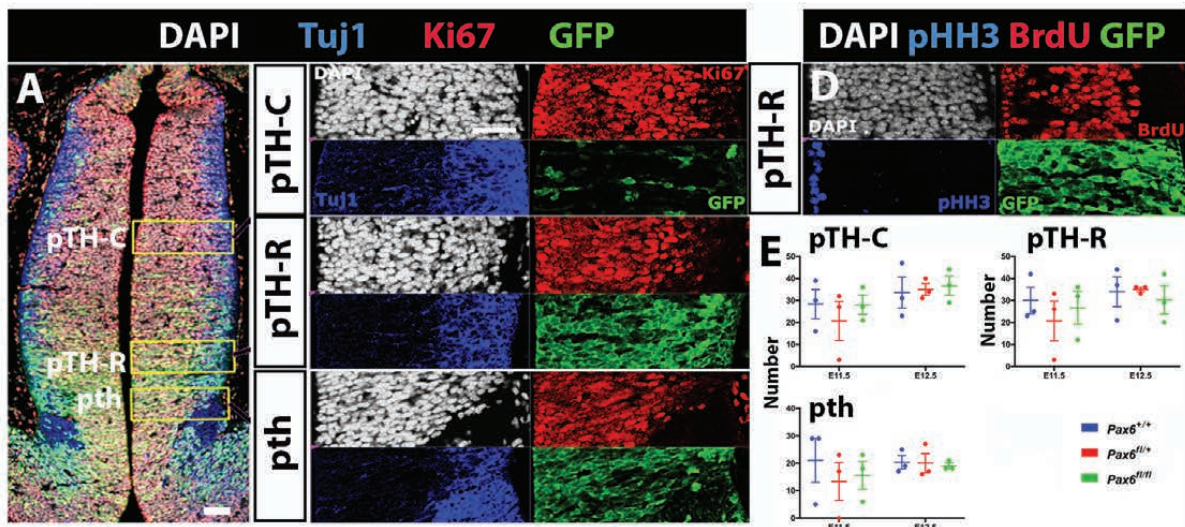


Proportion of VP cells born at different ages

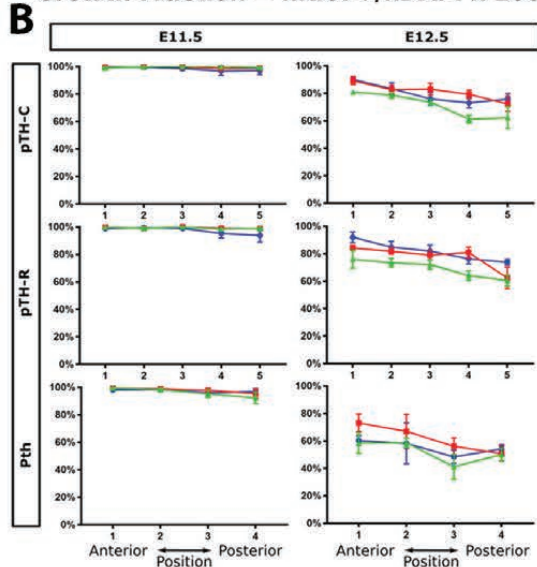


Proportion of GFP+ve VP cells born at different ages

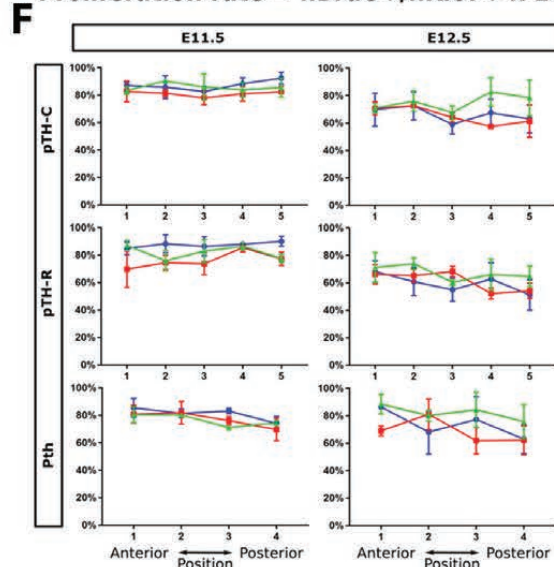




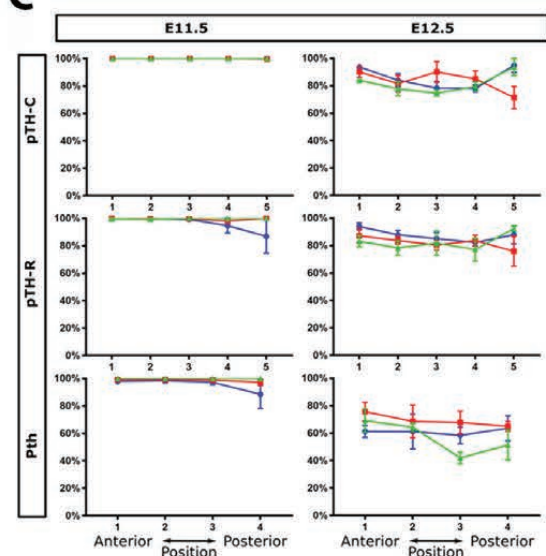
B Growth Fraction = $n\text{Ki67}+/n\text{DAPI} \times 100\%$



F Proliferation rate = $n\text{BrdU}+/n\text{Ki67}+ \times 100\%$



C GFP+ Growth Fraction



G GFP+ Proliferation rate

